IO1-1

Optimized Deep Learning Stacking Ensemble Model for Classification of Mandibular Defects on Panoramic Radiographs: A Transformative Approach for Prosthodontic Decision Support

〇Arwa Hammam Melhem，Mariko Hattori，Hiroyuki Shimizu，Noriyuki Wakabayashi
Department of Advanced Prosthodontics, Graduate School of Medical and Dental Sciences, Institute of Science Tokyo

[Objective]
To develop and evaluate an artificial intelligence framework for automatic classification of mandibular defects on panoramic radiographs according to the Cantor and Curtis system[1] by identifying optimal architectures through systematic evaluation of deep learning models and building an optimized stacking ensemble from top-performing networks
[Method]
Panoramic radiographs (n=400) were retrospectively collected from the Clinic for Maxillofacial Prosthetics, Institute of Science Tokyo Hospital (approval number: D2022-004) and classified into five defect types. Data were divided into 80% training and 20% validation sets. Preprocessing used Contrast-Limited Adaptive Histogram Equalization to enhance local contrast and an enriched data augmentation pipeline to improve robustness to imaging variability. Multiple architectures were trained and compared: CNNs (DenseNet201, EfficientNet-B1, ResNet50, ConvNeXt-Tiny), hybrid models (CoAtNet-0, MaxViT-Tiny), and transformers (Swin Transformer Tiny, DeiT-Small). Stratified 5-fold cross-validation was used to generate reliable out-of-fold predictions and address class imbalance, while Particle Swarm Optimization tuned hyperparameters (learning rate, batch size, epochs). Finally, a stacking ensemble was constructed using out-of-fold predictions of top-performing models as input features for a meta-learner trained to generate final class probabilities
[Results and Discussion]
DenseNet201 achieved the highest F1-score (0.869), followed by EfficientNet-B1 (0.857) and Swin Transformer Tiny (0.853), confirming architecture-dependent performance. The stacking ensemble surpassed single models with a precision of 0.911, recall of 0.912, and F1-score of 0.909, showing the advantage of integrating complementary features across CNN, hybrid, and transformer models. The ensemble improved stability in complex defect patterns, reducing misclassification in mandibular discontinuity (Fig. 1, 2). By providing reliable multi-class defect categorization directly from routine panoramic imaging, this AI-driven framework can standardize mandibular defect assessment, enhance prosthodontic decision-making, and support more objective design of rehabilitative prostheses in complex post-resection cases
[References]
1). Cantor R, Curtis TA. Prosthetic management of edentulous mandibulectomy patients. Part I. Anatomic, physiologic, and psychologic considerations. J Prosthet Dent 1971;25

（Name of approved Ethics Review Committee：Ethics Committee of the Faculty of Dentistry, Institute of Science Tokyo　Approval Number：D2022-004）

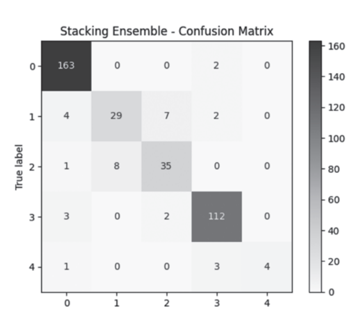

Figure 1: Confusion matrix for stacking ensemble model compares the true labels (rows) against the predicted labels (columns) to evaluate classification accuracy

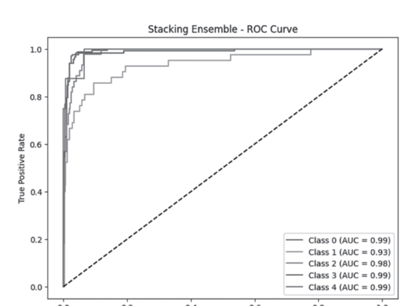

Figure 2: Receiver Operating Characteristic (ROC) curves for the stacking ensemble model visualizes the diagnostic ability of the multi-class classifier by mapping the true positive rate against the false positive rates at various threshold settings.

IO1-2

In vitro and numerical comparison of fracture behavior in resin-bonded fixed dental prosthesis

○Okkar Kyaw[1), Satoshi Yamaguchi[2), Hiraku Onuma[1), Manabu Kanazawa[1),
Masanao Inokoshi[3,4)

1) Department of Gerodontology and Oral Rehabilitation, Graduate school of medical and Dental Sciences, Institute of Science Tokyo,
2) AI Research Unit, Gruaduate School of Dentistry, The University of Osaka,
3) Department of Oral Devices and Materials, Graduate School of Medical and Dental Sciences, Institute of Science Tokyo,
4) Oral Science Center, Institute of Biomedical Engineering, Institute of Science Tokyo

[Objective]

This study aimed to directly compare the fracture behavior of resin-bonded fixed dental prostheses (RBFDPs) using *in vitro* testing and numerical simulations.

[Method]

The density of 5 mol% yttria-stabilized zirconia (5YSZ; KATANA Zirconia YML body 3, Kuraray Noritake Dental) was measured using Archimedes' method. Load-displacement curves (n=30) from four-point flexural strength tests, obtained from a previously published study[1], together with density measurements, were used to evaluate the input material properties of 5YSZ via numerical simulation of the four-point flexural strength test. A computer-aided design (CAD) model of an RBFDP was created based on typodont central and lateral incisors (standard practice model teeth; 18A5AN-500, Nissin). The scan data underwent geometric preprocessing in mesh editing software (Meshmixer, Autodesk) and a non-uniform rational B-splines (NURBS) format conversion within a CAD environment (Fusion 360, Autodesk).

The RBFDP CAD model was imported into a preprocessor (LS-PrePost, version 4.9, Ansys), and a nonlinear explicit dynamic finite element analysis was performed to evaluate the fracture resistance and biomechanical behavior of the RBFDP single compression analysis (RBFDP_SA). The maximum principal strain (MXEPS) distribution was recorded. The abutment and dental prosthesis were fabricated from the RBFDP CAD model by milling stainless steel and 5YSZ (KATANA Zirconia STML, Kuraray Noritake Dental). In vitro single-compression tests of the RBFDPs (RBFDP_ST) (n=3) were conducted using a universal testing machine (EZ-LX, Shimadzu). The fracture specimens were examined under a stereomicroscope and by scanning electron microscopy (SEM images), and the fracture features were compared with the MXEPS distribution obtained from RBFDP_SA.

[Results and Discussion]

The density and static elastic modulus of 5YSZ were 6.04 g/cm^3 and 101.85 GPa. The fracture resistance of RBFDP_SA was 348 N, whereas that of RBFDP_ST was 352 N. The predicted fracture resistance was within 5% of the experimental value. SEM observation revealed that the fracture origins in the experimental specimens corresponded to those predicted by the MXEPS distribution of RBFDP_SA. Overall, the fracture resistance and biomechanical behaviors of RBFDPs can be reliably predicted using numerical analysis.

[Reference]

Inokoshi M, Liu H, Yoshihara K, et al. Layer characteristics in strength-gradient multilayered yttria-stabilized zirconia. Dent Mater. 2023; 39(4): 430-41.

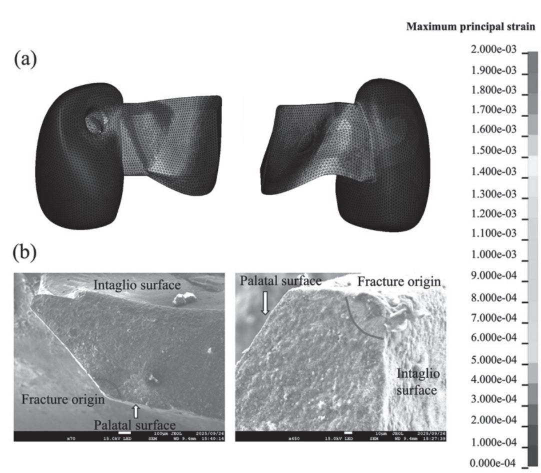

Figure 1. Fracture origins and crack pattern of resin-bonded fixed dental prosthesis (RBFDP). a) maximum principal strain distribution of the RBFDP; b) fractography by the scanning electron microscopy observation of the RBFDP.

IO1-3

Fabrication and Characterization of NIR-responsive Zirconia surface coated with Au/polydopamine.

○Hao Wu[1)], Kosuke Nozaki[1)], Masaya Shimabukuro[2)], Zhiwei Zhou[1)], Xiaohe Zhou[1)], Noriyuki Wakabayashi[1)]

[1)] Department of Advanced Prosthodontics, Institute of Science Tokyo,
[2)] Department of Inorganic Biomaterials, Laboratory for Biomaterials and Bioengineering, Institute of Integrated Research, Institute of Science Tokyo

Objective

Peri-implantitis is a prevalent and difficult-to-manage implant complication characterized by persistent inflammation, biofilm tolerance, and progressive alveolar bone loss. Recent advances in stimulus-responsive biomaterial surfaces have attracted considerable attention for the development of antibacterial and osteoconductive implants. Near-infrared (NIR) light is a particularly attractive stimulus because it can penetrate gingival tissue and aqueous environments, thereby enabling activation of embedded biomaterials in situ. This study aims to develop an NIR-responsive amorphous zirconia implant coating functionalized with polydopamine (PDA) and gold nanoparticles (Au) to achieve heat-mediated antibacterial potential.

Methods

PDA/Au-functionalized amorphous zirconia coatings on zirconia substrates were characterized by SEM/EDS, XRD, FTIR, UV–Vis spectroscopy, and contact angle analysis, while NIR responsiveness was assessed by monitoring temperature changes under NIR irradiation.

Results and Discussion

SEM analysis revealed uniform coating coverage with well-dispersed Au nanoparticles (average diameter is 10.7 nm), while EDS mapping confirmed homogeneous Zr and O distributions with Au localized at the surface. XRD patterns exhibited a weak Au(111) diffraction peak at approximately 38.2 degree, indicating successful Au nanoparticle formation. FTIR spectra verified polydopamine deposition on zirconia through characteristic –OH/–NH and carbonyl/aromatic bands, and UV–Vis spectroscopy showed a localized surface plasmon resonance peak at 520–540 nm, consistent with the nanoparticle size and PDA-assisted immobilization. Wettability measurements indicated a moderately hydrophilic surface, which is favorable for osteoblast adhesion and spreading while avoiding extremes of hydrophobicity or superhydrophilicity. NIR irradiation increased the temperature from 37 degree centigrade to 56 degree centigrade, whereas the control samples exhibited only a 4 degree centigrade increase. These results suggest that Au/polydopamine coatings have strong potential for fabricating NIR-responsive zirconia materials for antibacterial therapy.

References

Feng, K.; Wang, G.; Wang, S.; et al. Breaking the pH Limitation of Nanozymes: Mechanisms, Methods, and Applications. Advanced Materials 2024, 36 (31), 2401619.

IO2-1

Time-Dependent Extracellular Matrix Maturation During Osteoblastic Differentiation Revealed by Integrated Transcriptomic and Proteomic Analyses

○Hlaing Pwint Phyu，Azusa Dobashi，Mizuki Kobayashi，Yoshiki Ono，Masaru Kaku
Division of Bio-Prosthodontics, Faculty of Dentistry & Graduate School of Medical and Dental Sciences, Niigata University

[Objective]
Long-term success of prosthodontic treatments, particularly dental implant therapy, depends on proper bone quality, in which the extracellular matrix (ECM), the main organic constituent of bone, plays a central role. Although osteoblastic differentiation has been extensively investigated at the transcriptional level, how gene expression programs translate into ECM protein accumulation and maturation remains unclear. This study aimed to elucidate ECM maturation during osteoblastic differentiation by examining the temporal relationship between osteoblast gene expression and ECM deposition using an integrative transcriptomic and ECM-oriented proteomic approach.
[Method]
A mouse calvaria-derived pre-osteoblastic cell line (MC3T3-E1) was cultured for up to four weeks. Transcriptomic changes were analyzed by bulk RNA sequencing at weekly intervals. ECM composition was quantitatively analyzed using an ECM-focused proteomic workflow incorporating decellularization, hydroxylamine-based chemical digestion, deglycosylation, and LC–MS/MS analysis. Temporal changes in gene expression and ECM protein abundance were compared using integrative bioinformatic analyses.
[Results and Discussion]
Transcriptomic analysis revealed a major shift in gene expression between weeks 1 and 2, characterized by a transition from cell cycle–related pathways to osteoblast differentiation and ECM-associated pathways. In contrast, ECM proteomic analysis showed a progressive and cumulative increase in total ECM protein content throughout differentiation, despite relatively stable numbers of identified ECM proteins. Type I collagen predominated at all stages, whereas non-collagenous ECM proteins, including proteoglycans and ECM glycoproteins, exhibited distinct temporal remodeling patterns. Correlation analysis demonstrated weak concordance between mRNA expression and ECM protein abundance, indicating substantial temporal uncoupling between transcriptional regulation and matrix accumulation. Only a limited subset of proteins, such as PLOD1, PODN, and LAMB1, showed parallel transcript-level changes. These findings indicate that ECM maturation reflects cumulative osteoblastic activity rather than single-time-point gene expression. Collectively, the results highlight that bone quality is governed by time-dependent ECM maturation, providing a biological basis for understanding osseointegration, peri-implant bone stability, and long-term implant success.

日補綴会誌　18・135 回特別号，2026

IO2-2

Interface Engineering of 1.5YSZ Implants Using ABL-(Zn/Cu/Sr)-Tannic Acid Metal-Phenolic Networks

Sub Title: An In Vitro Study of Bioactivity and Osteogenesis

○Zhiwei Zhou，Kosuke Nozaki，Satsuki Tanaka，Hao Wu，Xiaohe Zhou，Noriyuki Wakabayashi
Advanced Prosthodontics, Division of Oral Health Sciences, Graduate School, Institute of Science Tokyo

[Objective]

1.5 mol% yttria-stabilized zirconia (1.5YSZ) possesses superior mechanical properties for dental implants but lacks bioactivity. Recent advances in interface engineering suggest that metal–phenolic networks (MPNs) provide a versatile platform for functional surface modification through supramolecular coordination chemistry.This study engineered multifunctional nano-coatings on 1.5YSZ using metal-phenolic networks (MPNs) incorporating tannic acid (TA), abaloparatide (ABL), and metal ions (Zn, Cu, Sr) [1]. Specifically, this study aimed to (i) construct stable ABL-loaded MPN coatings on 1.5YSZ surfaces, (ii) elucidate the effects of different metal ion combinations on surface physicochemical properties, and (iii) evaluate their influence on osteoblast viability, differentiation, and mineralization in vitro, with the goal of enhancing zirconia–bone integration.

[Method]

1.5YSZ discs were coated with TA-ABL complexes coordinated with metal ions, forming ABL@ZnTA (Zn), ABL@ZnCuTA (ZnCu), and ABL@ZnSrTA (ZnSr) groups. Surface characteristics were analyzed via scanning electron microscopy (SEM), energy dispersive X-ray spectroscopy (EDS), and Fourier transform infrared spectroscopy (FTIR). Osteoblast-like MC3T3-E1 cells were seeded to evaluate cytotoxicity (CCK-8), osteogenic differentiation (ALP activity), and mineralization (Alizarin Red S staining) over 28 days.

[Results and Discussion]

SEM and FTIR confirmed successful coating assembly, which improved hydrophilicity without cytotoxicity. While all coated groups enhanced osteogenesis compared to uncoated 1.5YSZ, the ZnSr group exhibited superior performance. The Zn group showed an early ALP peak followed by a rapid decline, whereas the ZnSr group maintained high ALP activity through Day 14, suggesting a prolonged window of osteogenic stimulation [2]. Consequently, ZnSr induced the most robust mineralization at Day 28. These findings indicate that ABL@ZnSrTA synergizes zirconia's stability with the bioactivity of ABL and strontium, offering a promising strategy for advanced implants [3].

[References]

1.Xu L, Fang J, Pan J, et al. Zinc finger-inspired peptide-metal-phenolic nanointerface enhances bone-implant integration. Bioact Mater 2024; 41.
2.Aimaiti A, Mai A, Boyong X, et al. Low-dose strontium stimulates osteogenesis but high-dose doses cause apoptosis. Stem Cell Res Ther 2017; 8.
3.Zhong Z, Wu X, Wang Y, et al. Zn/Sr dual ions-collagen co-assembly hydroxyapatite enhances bone regeneration. Bioact Mater 2022; 10.

IO2-3

In vitro evaluation of biocompatibility and osteoconductive potential of ultrashort pulsed laser–treated ceria-stabilized zirconia/alumina nanocomposite surfaces as material for dental implants.

○Bryan Martin del Campo[1], Minoru Sanda[1], Shoma Yamamori[1], Takahito Osawa[1], Yoko Oshima[1], Eri Urano-Morisawa[1], Ayako Mochizuki[2], Fuminori Iwasa[3], Kazuyoshi Baba[1]

[1] Department of Prosthodontics, Showa Medical University, School of Dentistry,
[2] Department of Oral Physiology, Showa Medical University, School of Dentistry,
[3] Division of Fixed Prosthodontics, Department of Restorative and Biomaterials Sciences, Meikai University, School of Dentistry

[Objective]
This study evaluated the surface characteristics and osteoconductive potential of ultrashort pulsed laser–treated ceria–stabilized zirconia/alumina (Ce-TZP/Al_2O_3) nanocomposite in vitro.
[Method]
Disk-shaped specimens (20.0 mm diameter, 1.0 mm thickness) made of Ce-TZP/Al_2O_3 were prepared. Untreated specimens with a machined surface served as controls, whereas the experimental specimens were subjected to ultrashort-pulsed laser surface texturing. The surface topography and chemical states were analyzed using scanning electron microscopy (SEM), atomic force microscopy (AFM), and X-ray photoelectron spectroscopy (XPS). Osteoconductive potential was evaluated using MC3T3-E1 pre-osteoblastic cells by measuring cell adhesion (3 and 24 hours), proliferation (5 days), and alkaline phosphatase (ALP) activity on days 7, 14, and 21 (n = 4). Osteogenic gene expression of type I collagen (Col1a1), osterix (Sp7), osteopontin (Spp1), and osteocalcin (Bglap) was analyzed by quantitative real-time polymerase chain reaction (qRT-PCR) at 3, 7, and 14 days (n = 3).
[Results and Discussion]
Control specimens exhibited smooth and flat surfaces, while laser-treated specimens showed micro- and nanostructured topography with greater surface area, roughness, and pronounced undercuts (1). In vitro assays demonstrated a significant increase in cell adhesion, proliferation, and ALP activity in laser-treated Ce-TZP/Al_2O_3nanocomposites compared with controls, and the qRT-PCR analysis indicated higher expression of osteogenic-related genes, with upregulation of Sp7 at day 3, Spp1 at days 3 and 7, and Bglap at days 7 and 14 (2).
Ultrashort pulsed laser–induced macro- and nanostructuring of Ce-TZP/Al_2O_3 surfaces significantly improved osteoconductive responses in vitro, suggesting its potential as a dental implant material.
[References]
1) Li Y, et al. Enhanced osteoconductivity of zirconia implants with one-step femtosecond laser treatment through morphological and chemical modifications. J Funct Biomater 2025; 16(4): 142.
2) Oshima Y, et al. Effect of nanofeatured topography on ceria-stabilized zirconia/alumina nanocomposite on osteogenesis and osseointegration. Int J Oral Maxillofac Implants 2017; 32(1): 81–91.